

A scanning tunneling microscopy study of the GaAs(112) surfaces

L. Geelhaar^{a,*}, J. Márquez^a, K. Jacobi^a, A. Kley^a, P. Ruggerone^b, M. Scheffler^a

^aFritz-Haber-Institut der Max-Planck-Gesellschaft, Faradayweg 4–6, 14195 Berlin, Germany

^bInstituto Nazionale per la Fisica della Materia, Università di Cagliari, Cagliari, Italy

Accepted 6 November 1998

Abstract

The GaAs(112)A and B surfaces were prepared by molecular beam epitaxy (MBE) and characterized in situ by scanning tunneling microscopy (STM). Both surfaces are unstable. On the (112)A surface five facets with the orientations {111}, {110} and {124} appear, while on the $(\bar{1}\bar{1}\bar{2})$ B surface four facets with the orientations $(\bar{1}\bar{1}\bar{1})$ B, $(\bar{1}\bar{1}\bar{0})$ and $(\bar{1}\bar{1}\bar{3})$ B were observed. In both cases, the facets form depressions covering the entire surface. In addition, total-energy calculations employing density-functional theory were carried out for these surfaces. For the (112)A surface a roof-like structure of {111} and {113} planes has the lowest calculated energy. According to the calculations, the $(\bar{1}\bar{1}\bar{2})$ B surface forms under As-rich conditions a roof-like structure of $(\bar{1}\bar{1}\bar{1})$ B and $(\bar{1}\bar{1}\bar{3})$ B planes, and it decomposes under Ga-rich conditions into $(\bar{1}\bar{1}\bar{0})$ planes. The experimental and theoretical findings for the $(\bar{1}\bar{1}\bar{2})$ B surface are in good agreement. The occurrence of {124}-facets on the (112)A surface was not taken into consideration in the calculations and needs to be investigated further. © 1999 Elsevier Science Ltd. All rights reserved.

Keywords: Gallium arsenide; High-index surfaces; Molecular beam epitaxy; Scanning tunneling microscopy; Total-energy calculations; Structure

1. Introduction

Recently, there has been an ever-increasing interest in the growth of self-organized low-dimensional quantum structures [1]. In addition to studies on low-index surfaces, research has been directed towards the potential benefit of high-index surfaces as substrates. Using metal organic vapor phase epitaxy (MOVPE), Nötzel et al. [2] grew InGaAs quantum disks on GaAs (311)B substrates. The preparation of aligned arrays of InGaAs quantum dots has been achieved on the same surface by employing hydrogen-assisted MBE [3] and gas-source MBE [4]. The formation of quantum dots has also been observed on GaAs (311)A [5]. Guo et al. [6] reported the MBE growth of InAs quantum dots and quantum dashes on GaAs (211)B. From photoluminescence emission measurements Lubyshev et al. [7] determined the quantum efficiency in InGaAs quantum dots on various low- and high-index GaAs surfaces and found the highest value on (711)B.

The particular physical properties of high-index surfaces can be exploited not only by using them as substrates for quantum structures but also for other applications. For example, the (211)B surface has been found to be the

optimum direction for second-harmonic surface emission structures [8,9].

In order to understand better and thus be able to optimize the growth of the desired structures, a combined experimental and theoretical study of the bare surfaces is necessary. In this article we present such a study on the GaAs (112)A and B surfaces.

The (112) surfaces are particularly interesting among the high-index orientations because the first layer of the bulk-truncated structure contains an equal number of cations and anions.

So far only diffractive techniques have been used to examine in situ the structure of the GaAs (112) surfaces. Ranke [10] observed on a cylindrical MBE-prepared GaAs single crystal in the (112) direction strong faceting of the low energy electron diffraction (LEED) spots and concluded that the surface consists of $(10\bar{1})$ and $(01\bar{1})$ facets. Hren et al. [11] studied, also by means of LEED, the two inequivalent (211) surfaces prepared by an etch-heat-cleaning (EHC) method and by the ion-bombardment annealing (IBA) technique. However, these authors were not able to determine which surface was the A and which was the B face, respectively. On one surface, they observed a decomposition into two different {110} facets, and on the other a decomposition into three {110} facets. Nötzel et al. [12] used reflection high-energy electron diffraction (RHEED) to investigate the structure of the MBE-prepared (211)A surface. A

* Corresponding author.

E-mail address: geelhaar@fhi-berlin.mpg.de (L. Geelhaar)

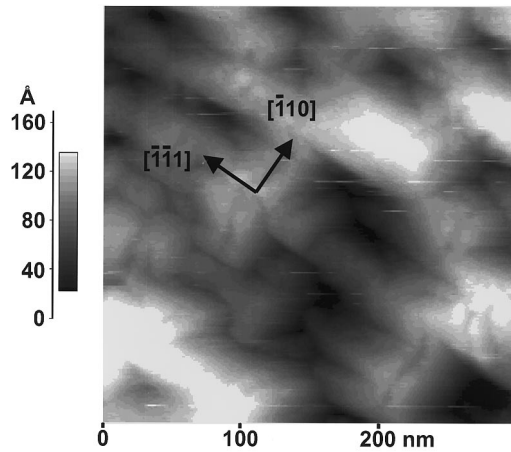


Fig. 1. STM-image of the GaAs(112)A surface. Tunneling current 0.2 nA, sample bias -2 V.

reversible transition between a flat surface showing a high degree of disorder below 550°C and a regular faceted surface above 590°C was found. The faceted surface is formed from asymmetrical pyramids consisting of two $\{110\}$ facets, (111) terraces and (001) steps. Most recently, our group carried out a spot-profile analysis LEED (SPA-LEED) study on both the $(112)\text{A}$ and B surfaces prepared by MBE [13]. The $(112)\text{A}$ surface decomposes into five kinds of facets with the orientations $\{110\}$, $\{124\}$ and (111) . The $(\bar{1}\bar{1}\bar{2})\text{B}$ surface comprises only four kinds of facets, namely $(\bar{1}\bar{1}\bar{1})\text{B}$, $(\bar{1}\bar{1}\bar{3})\text{B}$ and $(\bar{1}\bar{1}\bar{0})$. These results have been partly further confirmed by an ex situ atomic force microscopy (AFM) study and theoretical calculations, which are also included in the present contribution [14].

To our knowledge only one article has been published on theoretical efforts to predict the structure of the GaAs(112) surfaces. According to Chadi's calculations [15], the average of the surface energies of the two (112) surfaces is three times larger than the surface energy of the (110) face, suggesting an instability with respect to faceting.

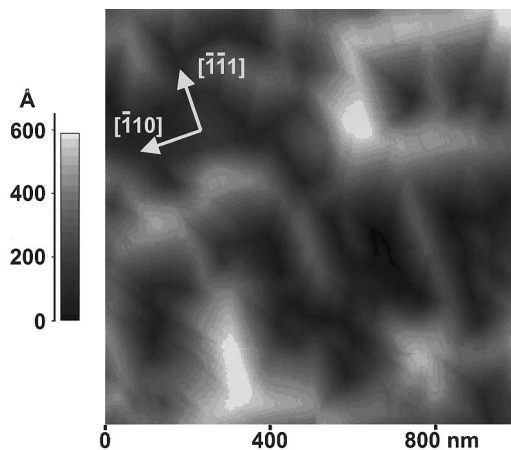


Fig. 2. STM-image of the GaAs $(\bar{1}\bar{1}\bar{2})\text{B}$ surface. Tunneling current 0.3 nA, sample bias -2 V.

The aim of our research is, on the one hand, to fill the gap in the previous experimental studies and to present the first in situ, real-space images of the GaAs(112) surfaces. This has been done by preparing the samples with MBE and examining the surface structure in situ with a scanning tunneling microscope (STM). On the other hand, ab initio total energy calculations were carried out for both inequivalent faces in order to derive the surface structure on a theoretical basis.

2. Experimental

2.1. Methods

Experiments were carried out in a multiple-chamber UHV-system. In our standard procedure samples are prepared by MBE and can be examined in situ by the following techniques of surface analysis: STM, RHEED, LEED and photoemission. The samples used in this study were cleaned with propanol and introduced into the UHV-system via a load lock. Before deposition they were degassed and subjected to several ion-bombardment annealing (IBA) cycles. During the MBE-process, the sample temperature was measured with an IR-pyrometer and kept at 540°C . The $\text{As}_4:\text{Ga}$ ratio was 10, and at growth rates of about 1 \AA/s the thickness of the layers grown was ca. 50–100 nm. A more detailed description can be found elsewhere [13].

Real-space images were taken with a commercially available STM (VP2, Park Scientific Instruments). The sample holder was modified to fit our UHV-transfer system. Images were acquired in constant-current mode with tunneling currents between 0.2 nA and 0.3 nA and sample biases between -2 V and -3 V.

2.2. Results and discussion

An STM-image of the GaAs(112)A surface is shown in Fig. 1. It is clearly seen that the whole surface is faceted and that there are no flat areas with (112) orientation. Among the facets, five different planes can be distinguished. The facets form depressions in the surface whose horizontal cross-section is an irregular pentagon along $(\bar{1}\bar{1}\bar{1})$ and $(\bar{1}\bar{1}\bar{0})$. The depressions are not ordered, and their dimensions vary between 30 nm and 90 nm along $(\bar{1}\bar{1}\bar{0})$ and between 50 nm and 200 nm along $(\bar{1}\bar{1}\bar{1})$.

In Fig. 2 the corresponding picture for the $(\bar{1}\bar{1}\bar{2})\text{B}$ face is presented. The same observations are made as for $(112)\text{A}$, but there are only four different facets. Thus, rectangular depressions, $100\text{--}300 \text{ nm} \times 100\text{--}450 \text{ nm}$, are formed. These lie with their generally longer edge parallel to $(\bar{1}\bar{1}\bar{1})$ and with their generally shorter edge parallel to $(\bar{1}\bar{1}\bar{0})$.

On each surface, the number of different facet orientations is the same as reported in reference [13]. In order for the orientations of the facets to be identified, their angles with the horizontal were extracted from the STM-images

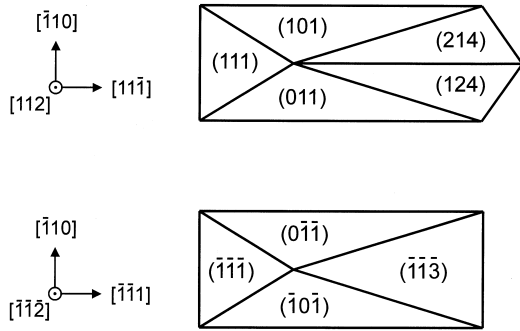


Fig. 3. Models for the depressions observed on the GaAs(112)A (upper part) and on the GaAs $(\bar{1}\bar{1}\bar{2})$ B surface (lower part).

and were averaged over many facets. Combining the facet orientations found in reference [13] with the real-space images of this work results in the models for the depressions that are depicted in Fig. 3. The experimental and ideal values for the angles are compared in Table 1. They are in good agreement. Hence, the STM-data confirm that on the GaAs(112)A surface facets with the orientations (111), $\{110\}$ and $\{124\}$ occur and that the $(\bar{1}\bar{1}\bar{2})$ B face decomposes into $(\bar{1}\bar{1}\bar{1})$ B, $(\bar{1}\bar{1}\bar{0})$ and $(\bar{1}\bar{1}\bar{3})$ B facets.

3. Theoretical

3.1. Methods

The surface free energy was calculated for a variety of reasonable surface models. The predicted stable structure is the one with the lowest value of this energy.

As the crystal considered is formed by two different elements the stoichiometry of the surface has to be taken into account in addition to the atomic geometry. This was done by allowing the surface to exchange atoms with a reservoir which is characterized by the chemical potential μ . The surface free energy γ_{surface} of the surface area A is defined by

$$\gamma_{\text{surface}}A = E_{\text{surface}} - \mu_{\text{Ga}}N_{\text{Ga}} - \mu_{\text{As}}N_{\text{As}}$$

where N_i denotes the number of atoms of the respective element. For the computations, the surface was represented

Table 1
Comparison between the experimentally found angles between the facet planes and the surface and the ideal values

GaAs(112)A					
Facet plane	(101)	(011)	(111)	(214)	(124)
Ideal angle	30°	30°	19.5°	11.5°	11.5°
Experimental	14°	15°	14°	12°	10°
GaAs $(\bar{1}\bar{1}\bar{2})$ B					
Facet plane	$(0\bar{1}\bar{1})$	$(\bar{1}0\bar{1})$	$(\bar{1}\bar{1}\bar{1})$	$(\bar{1}\bar{1}\bar{3})$	
Ideal angle	30°	30°	19.5°	10°	
Experimental	23°	22°	23°	16°	

by periodically repeated slabs. The surface energy was determined from the total energy E_{tot} of a slab. E_{tot} was calculated at zero temperature and zero pressure, and neglecting zero point interactions, by using density-functional theory (DFT). For the exchange-correlation functional the local density approximation (LDA) was employed.

Chemical equilibrium requires $\mu_{\text{Ga}} + \mu_{\text{As}} = \mu_{\text{GaAs}}$ where μ_{GaAs} is the bulk chemical potential. Thus, μ_{Ga} can be eliminated, yielding

$$\gamma_{\text{surface}}A = E_{\text{tot}} - \mu_{\text{GaAs}}N_{\text{Ga}} - \mu_{\text{As}}(N_{\text{As}} - N_{\text{Ga}}).$$

Changing the As_4 :Ga ratio in an MBE experiment corresponds to varying μ_{As} in this formula, assuming slow growth always close to thermal equilibrium with the gas phase. The permitted value range for μ is determined by $\mu_{\text{As}} < \mu_{\text{As}}^{\text{bulk}}$ and $\mu_{\text{Ga}} < \mu_{\text{Ga}}^{\text{bulk}}$. If the chemical potential exceeded the value for the condensed phase of the respective element, this elemental phase would form on the surface. A more comprehensive explanation and computational details can be found elsewhere [16].

3.2. Results and discussion

The results of the calculations are shown in Fig. 4, and the descriptions of the respective surface models are summarized in Table 2. In addition to reconstructions,

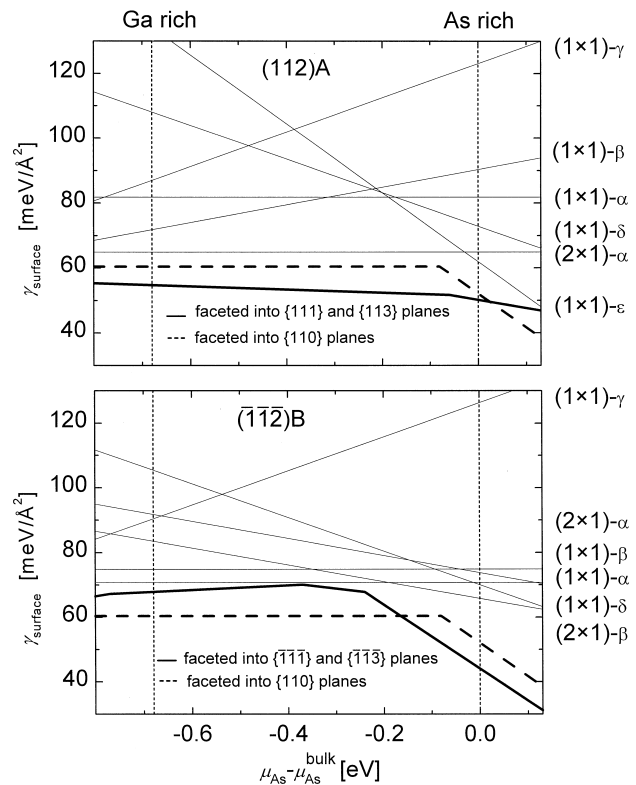


Fig. 4. Calculated free surface energies of the GaAs(112)A (upper part) and GaAs $(\bar{1}\bar{1}\bar{2})$ B surface (lower part) as a function of the As chemical potential. The surface models are described in Table 2.

Table 2

Structure models for the GaAs(112)A $[(\bar{1}\bar{1}\bar{2})\text{B}]$ surface, for which surface free energies have been calculated. The starting structure, which was relaxed in the ab initio calculations, is described

Name	Description
$(1 \times 1)\text{-}\alpha$	Truncated bulk structure
$(1 \times 1)\text{-}\beta$	As $(1 \times 1)\text{-}\alpha$ but 1st layer As[Ga] removed
$(1 \times 1)\text{-}\gamma$	as $(1 \times 1)\text{-}\alpha$ but 1st layer As substituted by Ga
$(1 \times 1)\text{-}\delta$	as $(1 \times 1)\text{-}\alpha$ but 1st layer Ga substituted by As
$(1 \times 1)\text{-}\epsilon$	as $(1 \times 1)\text{-}\alpha$ but 1st and 2nd layer Ga substituted by As
$(2 \times 1)\text{-}\alpha$	as $(1 \times 1)\text{-}\alpha$ plus As[Ga] dimer formation along $[\bar{1}10]$
$(2 \times 1)\text{-}\beta$	as $(1 \times 1)\text{-}\beta$ plus As dimer formation along $[11\bar{1}]$

faceted structures assembled according to Herring's construction were considered. For both orientations, faceting lowers the surface energy under all chemical conditions, and hence the GaAs(112) surfaces are unstable.

On the $(\bar{1}\bar{1}\bar{2})\text{B}$ face $\{110\}$ planes are formed in an As-rich environment while Ga-rich conditions yield faceting into $(\bar{1}\bar{1}\bar{1})\text{B}$ and $(\bar{1}\bar{1}\bar{3})\text{B}$ planes. This is in good agreement with the experiments where all four planes were observed on the same surface. This situation corresponds to a value for $\mu_{\text{As}} - \mu_{\text{As}}^{\text{bulk}}$ near the intersection between the dashed and the thick solid lines in the diagram.

For the (112)A surface a roof-like structure consisting of (111) and (113) planes has the lowest energy under all chemical conditions. However, at the As-rich end of the diagram the curve describing faceting into $\{110\}$ planes lies only slightly higher. The energy difference is smaller than the estimated margin of error. Thus, $\{110\}$ facets as observed in the experiments are not excluded by the calculations. Structures containing $\{124\}$ planes were not taken into consideration in the computations. There is agreement between theory and experiment in that the surface is not stable but decomposes into facets. The unexpected occurrence of $\{124\}$ planes needs to be investigated further.

4. Conclusions

STM experiments and ab initio total-energy calculations showed that the GaAs(112)A and B surfaces are unstable and faceted. For the $(\bar{1}\bar{1}\bar{2})\text{B}$ face, four kinds of facets with the orientations $(\bar{1}\bar{1}\bar{1})\text{B}$, $\{110\}$ and $(\bar{1}\bar{1}\bar{3})\text{B}$ were both found by experiment and predicted by theory. According to the STM data, five kinds of facets with the orientations (111),

$\{110\}$ and $\{124\}$ are present on the (112)A face. These facets were also suggested by the computations, with the exception of the $\{124\}$ planes, which were not taken into consideration.

The occurrence of the high-index facets $(\bar{1}\bar{1}\bar{3})\text{B}$ and $\{124\}$ should be especially noted. This finding suggests that they are low-energy surfaces and could be suitable substrates for quantum structures. Also, these orientations should be taken into consideration as potentially enveloping surfaces of quantum structures. In particular, further studies of GaAs(124) could yield interesting results.

Acknowledgements

We would like to thank Peter Geng for technical assistance. This work was supported by the Deutsche Forschungsgemeinschaft (Sonderforschungsbereich 296, Projects A2 and A5) and by the German Bundesministerium für Bildung und Forschung under grant No. 05 622 EBA4.

References

- [1] H. Asahi, Adv. Mater 9 (1997) 1019.
- [2] R. Nötzel, J. Temmyo, T. Tamamura, Nature 369 (1994) 131.
- [3] Y.J. Chun, S. Nakajima, M. Kawabe, Jpn. J. Appl. Phys. 35 (1996) L1075.
- [4] K. Nishi, T. Anan, A. Gomyo, S. Kohmoto, S. Sugou, Appl. Phys. Lett. 70 (1997) 3579.
- [5] R. Nötzel, Z. Niu, M. Ramsteiner, H.-P. Schönherr, A. Transpert, L. Däweritz, K.H. Ploog, Nature 392 (1998) 56.
- [6] S.P. Guo, H. Ohno, A. Shen, F. Matsukura, Y. Ohno, Appl. Phys. Lett. 70 (1997) 2728.
- [7] D.I. Lubyshev, P.P. González-Borrero, E. Marega Jr, E. Petitprez, P. Basmaji, J. Vac. Sci. Technol. B14 (1996) 2212.
- [8] N.D. Whitbread, J.S. Roberts, P.N. Robson, M.A. Pate, Electron. Lett. 29 (1993) 2106.
- [9] P.A. Ramos, E. Towe, Appl Phys. Lett. 69 (1996) 3321.
- [10] W. Ranke, Physica Scripta T4 (1983) 100.
- [11] P. Hren, D.W. Tu, A. Kahn, Surface Sci. 146 (1984) 69.
- [12] R. Nötzel, L. Däweritz, K. Ploog, Phys. Rev. B46 (1992) 4736.
- [13] J. Platen, C. Setzer, P. Geng, W. Ranke, K. Jacobi, Microelectronics Journal 28 (1997) 969.
- [14] J. Platen, A. Kley, C. Setzer, K. Jacobi, P. Ruggerone, M. Scheffler, submitted to J. Appl. Phys.
- [15] D.J. Chadi, J. Vac. Sci. Technol. B3 (1985) 1167.
- [16] N. Moll, A. Kley, E. Pehlke, M. Scheffler, Phys. Rev. B 54 (1996) 8844.